# Orientation of Pyrylium Guests in Cucurbituril Hosts

Arumugam Thangavel, Chariklia Sotiriou-Leventis,* Richard Dawes,* and Nicholas Leventis*

Department of Chemistry, Missouri University of Science and Technology, Rolla, Missouri 65409, United States

S *Supporting Information*

ABSTRACT: According to recent reports, supramolecular complexes of the pyrylium cation with cucurbit[x]urils (CB[x], x = 7, 8) show promising photoluminescence suitable for electroluminescent devices. In turn, photoluminescence seems to be related to the stereochemistry of the complexes; however, that has been controversial. Here, we report that in H$_2$O, 2,6-disubstituted-4-phenyl pyryliums (**Pylm**) form dimers quantitatively (equilibrium constants >10^4 M^{-1}), but they enter as such only in the larger **CB[8]**. In terms of orientation, ^{1}H NMR shows that **Me-Pylm**, **Ph-Pylm**, and **t-Bu-Pylm** insert their 4-phenyl groups in either the **CB[7]** or **CB[8]** cavity. The orientation of **iPr-Pylm** in the **iPr-Pylm@CB[7]** complex is similar. Experimental conclusions are supported by DFT calculations using the M062X functional and the 6-31G(d) basis set. In the case of (**iPr-Pylm**)$_2$**@CB[8]**, ^{1}H NMR of both the guest and the host indicates that both guests might enter **CB[8]** from the same side with their *iPr* groups in the cavity, but DFT calculations leave room for ambiguity. In addition to the size and hydrophobicity of the 2,6-substituents of the guests, as well as the size and flexibility of the hosts, theory reveals the importance of explicit solvation (H$_2$O) and finite temperature effects (particularly for ^{1}H NMR shielding calculations) in the determination of the stereochemistry of those complexes.
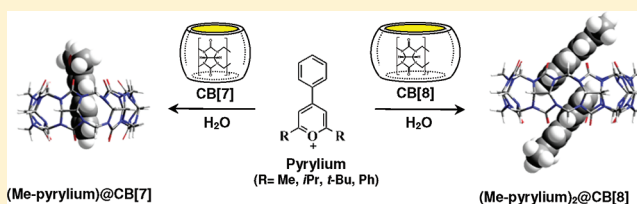
INTRODUCTION

Cucurbit[x]urils (CB[x]s) are water-soluble, barrel-shaped hosts prepared by condensation of x mol of glycoluril and 2x mol of formaldehyde.[1] The two portals are formed by the glycoluril carbonyl groups. X-ray crystallography shows a similar cavity height (distance between the O-atoms of the two rims) for all x (~6.1 Å), and portal diameters that vary with x, from 5.40 Å for **CB[5]** to 10.3 Å for **CB[8]**.[1−3]

CB[x]s show affinity for cationic guests, and dications with lengths matching the interportal distance have been studied extensively. For example, *N,N′*-dimethylviologen (with N–N distance of 7.3 Å) stretches the 4,4′-dipyridyl moiety along the axis of the barrel, placing the positive N's near the negative rim O's of **CB[7]**.[9] However, when the *N*-substituents are larger and hydrophobic (e.g., *N,N′*-dibenzyl- or *N,N′*-di-*n*-butyl-viologen), they are the ones found inside the cavity, rather than the 4,4′-dipyridyl moiety.[10,11] By analogy, monocationic *N*-substituted-4-benzoylpyridinium guests can be oriented *exo* or *endo*, placing the most hydrophobic group inside the **CB[7]** cavity while the pyridinium N stays always close to the rim O's.[12,13] Interestingly, when the most hydrophobic group is the 4-benzoyl moiety itself, hydrophobic interactions seem to be strong enough to shift the keto/*gem*-diol equilibrium of the benzoyl C=O toward its keto form, forfeiting H-bonding with the solvent (H$_2$O). Reportedly, larger cavities, e.g., **CB[8]**, can accommodate two 1-e reduced *N,N′*-dimethylviologen cation radicals.[14]

In view of the above, it is recognized herewith that the relatively easy synthetic access of the 2,6-positions of the monocationic 4-phenylpyrylium system allows wide variation of the hydrophobicity, shape, and size of the guest that, together with the size of the cavity, permits a global survey of the factors at play in the stereochemistry of host−guest complexes with CB[x]s. For this, we consider the following four guests and proceed using a combination of experiment and computation.
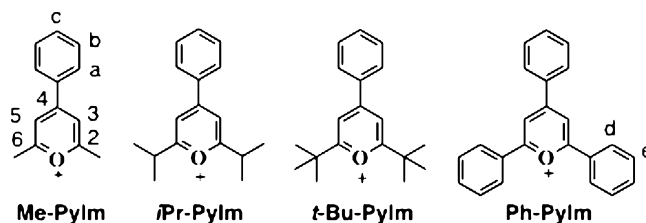
The 4-phenylpyrylium cation has been used for studying intercalation in cyclodextrins, showing an increasing preference for the hydrophobic interior of the host as hydrophobic substituents at the *c*-position of the 4-phenyl ring become longer.[15] In cucurbiturils, **Ph-Pylm** again places its 4-phenyl group inside the cavity and forms even more stable complexes due to additional electrostatic interactions with the portal C=O's.[16] In that regard, Montes-Navajas et al. argued that the size of CB[x] plays an important role in the relative mobility of the 2,6-phenyl groups: on the basis of molecular mechanics, they suggested that **Ph-Pylm** does not get as deep in **CB[7]** as in **CB[8]**, and once in **CB[7]**, the tight fit restricts rotation of the 4-phenyl group, while rotation of the 2- and 6-phenyl groups is free. In the same study, for the case of **CB[8]**, modeled rotation of the 4-phenyl group inside the cavity is free, while rotation of

the 2,6-phenyl groups is inhibited by the portal oxygens that frustrate the H_d's. The restricted rotation was thought to slow relaxation of an excited state, with the guest showing long-wavelength room temperature emission, which was attributed to phosphorescence and has been explored in electroluminescent devices.[16] Subsequently, however, that model was revised on the basis of the crystal structure of the **Ph-Pylm** complex with **CB[8]** showing that actually two **Ph-Pylm** moieties enter the host, both from the same side, in a parallel orientation, inserting either the 2- or the 4-phenyl groups into the cavity.[17] Clearly, those results warrant a thorough examination of the CB[x]-pyrylium system, not only for its possible utility but also for its basic stereochemistry. It is hereby reported that in H_2O, all four pyryliums shown above exist in equilibrium with their dimers and form preferentially 1:1 complexes with **CB[7]** and 2:1 complexes with **CB[8]**. In **CB[7]**, all four guests intercalate with the 4-phenyl group inside the cavity. In **CB[8]**, either antiparallel (**Me-**, **t-Bu-**) or parallel (**Ph-Pylm**) dimers of the pyryliums orient with the 4-phenyl groups inside the cavity. However, the stereochemistry of (**iPr-Pylm**)$_2$@**CB[8]** remains somewhat ambiguous, indicating the importance of explicit solvation in the orientation of those complexes.

■ RESULTS AND DISCUSSION

Synthesis of the BF_4^- salts of the four guests was carried out according to literature procedures,[18,19] and their identities were confirmed spectroscopically (see Experimental Section). ESI-MS[20] suggests that all four guests tend to form dimers (Figure 1). Absorption spectra in unbuffered water (pH ~2−4; more in
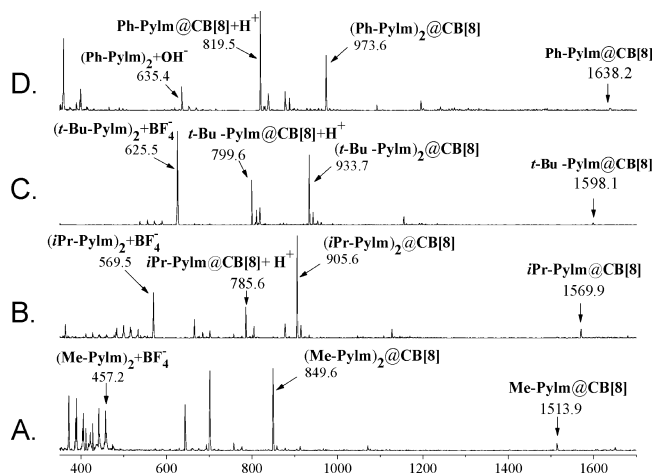

Figure 1. ESI-MS data with freshly made samples of the four guests in H_2O (~10^{-5} M) and ~1:1 mol/mol of **CB[8]**. (A) **Me-Pylm**; (B) **iPr-Pylm**; (C) **t-Bu-Pylm**; (D) **Ph-Pylm**.

conjunction with the discussion of ^{1}H NMR below) as a function of concentration (e.g., Figure 2 for **iPr-Pylm**) generally move to longer wavelengths and the intensity changes (J-aggregation).[21] Dimerization equilibrium constants (K_d, Table 1) were calculated spectrophotometrically by fitting data like those shown in Figure 2, inset (see also Section 2 in the Supporting Information).[22] It is noted that similar ε versus pyrylium concentration data (Figure 2, inset) should be also expected from isodesmic polymerization;[23] however, ESI-MS shows no higher aggregates beyond dimers. Experimental K_d values show near quantitative dimerization at room temperature
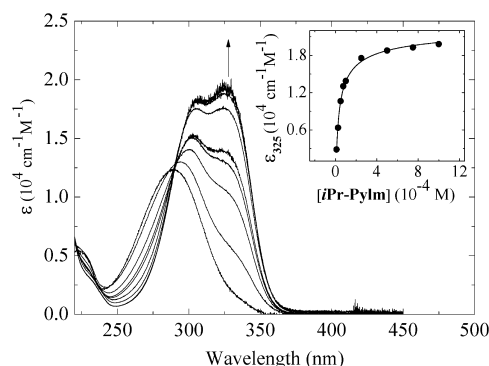

Figure 2. Absorption of a guest (**iPr-Pylm**) as a function of its concentration in H_2O. The red-shift is attributed to J-aggregation. Inset: nonlinear fit ($R^2 = 0.992$) of the extinction coefficient, ε, at 325 nm versus concentration.

and increase with the hydrophobicity (size) of the 2,6-substituents.

Dimerization is supported by density functional theory (DFT) calculations. Lowest energy fully relaxed dimer structures were located for all four guests of this study using the Gaussian 09 package with the Polarizable Continuum Model (PCM) for solvation (water) and the B3LYP or M062X levels of theory.[24] The latter is a more recent functional specifically designed for noncovalent interactions.[25,26] All calculations included the BF_4^- counterions, whose importance (and close association) to the electronic structure of pyrylium cations has been noted previously.[27] Dimers (**Me-Pylm**)$_2$, (**iPr-Pylm**)$_2$, and (**t-Bu-Pylm**)$_2$ prefer the head-to-tail (antiparallel) orientation by both the B3LYP and the M062X methods. In the case of (**Me-Pylm**)$_2$ we have been able to grow crystals, and X-ray analysis confirms the antiparallel orientation predicted by theory. (Crystallographic and calculated structures are provided in Sections 6 and 7, respectively, of the Supporting Information.) On the other hand, (**Ph-Pylm**)$_2$ prefers an antiparallel (head-to-tail) configuration at the B3LYP level but adopts a slipped head-to-head (parallel) π-stacking type of arrangement with the M062X functional, similar to the arrangement identified in the crystal structure of (**Ph-Pylm**)$_2$@**CB[8]**.[17] Importantly, despite similar dimer structures for three of the guests, the M062X method predicts much larger dimerization energies (included in Table 1). Gibbs free energies at 298 K (ΔG^{298}) estimated via harmonic frequency calculations were used to compute relative concentrations of dimers and, from those, dimerization constants (Table 1). Uncertainty in the calculated energies is due to the level of theory, the implicit solvent model, and the use of the harmonic-oscillator rigid-rotor model to estimate finite temperature effects. Despite those limitations, the M062X K_d values are in reasonably good agreement with the experimental ones, though the latter show even more favored dimerization than the M062X predictions. On the other hand, although B3LYP predicts generally similar 0 K structures (except for (**Ph-Pylm**)$_2$), it yields negligible dimerization at 298 K (Table 1).

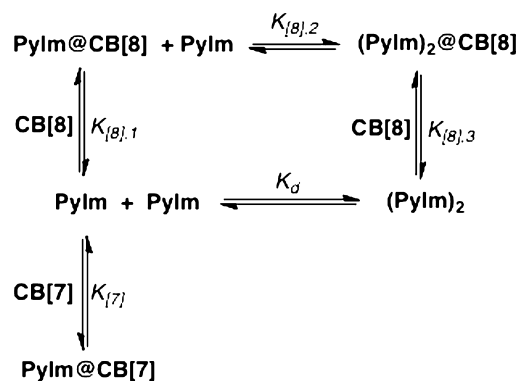Spectrophotometric Job's plots[28] clearly show that all four guests form 1:1 complexes with **CB[7]** (see Figure S1-A in Supporting Information). Similar Job's plots for the **CB[8]** complexes are ambiguous (Figure S1-B) and hence of low interpretational value in this case.[28d,e] ESI-MS though (Figure 1) shows that all guests form 2:1 complexes with **CB[8]**; in all cases the 1:1 complexes are also present, but the 2:1 peaks are

Table 1. Dimerization Data for the Four Pyrylium Guests of This Study in Water[a]

	K_d, M^{-1} [ΔG^{298}, kcal mol^{-1}]		
guest	experimental	B3LYP	M062X
Me-Pylm	1.0×10^4 [-5.45^b]	1.0×10^{-5} [6.81]	1.2×10^3 [-2.11]
*i*Pr-Pylm	3.2×10^4 [-6.14^b]	4.9×10^{-7} [8.61]	1.5×10^4 [-2.85]
t-Bu-Pylm	1.2×10^5 [-6.92^b]	9.6×10^{-7} [8.22]	4.2×10^3 [-2.48]
Ph-Pylm	3.9×10^5 [-7.62^b]	5.3×10^{-5} [5.84]	2.7×10^3 [-2.34]

[a]pH ~2−4. [b]Calculated from the experimental K_d values via $\Delta G^{298} = -RT \ln(K_d)$ (T = 298 K).

stronger (except for **Ph-Pylm@CB[8]**, where that trend is reversed). Meanwhile, the phosphorescence-based Job's plot for the **Ph-Pylm/CB[8]** system in ref 17 shows a clear maximum at $X = 0.5$ (X: relative mol fraction of **Ph-Pylm**). In view of other related reports,[29] that should be considered as a strong indication that phosphorescence comes exclusively from **Ph-Pylm@CB[8]**, which does not preclude equilibrium with nonphosphorescent **(Ph-Pylm)₂@CB[8]** (a case of concentration quenching). Putting all this information together, we postulate two mechanisms for intercalation in **CB[8]**, one stepwise and one where guests enter directly as dimers (Scheme 1).

Scheme 1. Intercalation Mechanism of Me-, *i*Pr-, *t*-Bu-, and Ph-Pylm in CB[7] and CB[8]

Pylm@CB[8] + Pylm $\underset{}{\overset{K_{[8],2}}{\rightleftharpoons}}$ (Pylm)₂@CB[8]

CB[8] $\Big\| K_{[8],1}$ CB[8] $\Big\| K_{[8],3}$

Pylm + Pylm $\underset{}{\overset{K_d}{\rightleftharpoons}}$ (Pylm)₂

CB[7] $\Big\| K_{[7]}$

Pylm@CB[7]

Equilibrium constants $K_{[7]}$, $K_{[8],1}$, and $K_{[8],2}$ (Table 2) were calculated via spectrophotometric titrations (e.g., Figure 3 and Section 3 in the Supporting Information).[30] $K_{[7]}$ decreases monotonically from **Me-Pylm** to **Ph-Pylm**, presumably reflecting crowding, namely, bulkier substituents prevent pyrylium from going as deep, and those complexes do not realize maximum stabilization. With regards to **CB[8]**, although a similar trend is not readily identifiable with $K_{[8],1}$, $K_{[8],2}$ does follow an analogous trend with $K_{[7]}$, again presumably because of crowding. Further, $K_{[8],2} > K_{[8],1}$, that is, once the first pyrylium has entered the larger **CB[8]** cavity, there is a significant driving force to take up a second guest. Nevertheless, the value-difference between $K_{[8],1}$ and $K_{[8],2}$ decreases from **Me-** to **Ph-Pylm** owing to the downward trend of $K_{[8],2}$, again following increased crowding as 2,6-substituents become larger.
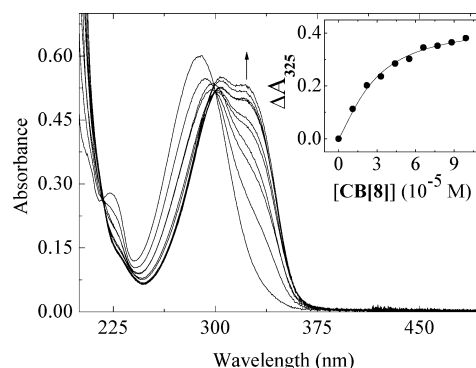

Figure 3. Spectrophotometric titration in unbuffered H₂O (pH ~2−4) of **Me-Pylm** (4.74 × 10^{-5} M) with **CB[8]**. Multiple spectral intersections reflect multistep processes (Scheme 1). Inset: nonlinear fit (R^2 = 0.990) of absorbance as indicated.

Overall, $K_{[8],3}$ values (calculated via $K_{[8],3} = K_{[8],1}K_{[8],2}/K_d$), which might have been expected to follow the same trend as $K_{[7]}$, show an interesting trend-reversal at **(*i*Pr-Pylm)₂@CB[8]**, implying a larger driving force for intercalation. That might be explained by a change in stereochemistry, and becomes a focal point in the following discussion.

Attempts to grow crystals of host−guest complexes and particularly of **(*i*Pr-Pylm)₂@CB[8]** were unsuccessful. For their stereochemistry we rely on ¹H NMR and calculations by the M062X/6-31G(d) method. Efforts to reproduce the ¹H NMR spectra computationally have set the reliability limit for calculations and provide useful insight on global factors at play in the intercalation of pyrylium guests in CB[*x*] hosts.

¹H NMR of guests, typically in D₂O, has been used as a reliable tool for structural elucidation of host−guest complexes with CB[*x*]s.[9−14] H's inside the cavity move upfield, while H's outside and near the rim O's move downfield. Figure 4 shows the evolution of the spectra of **Me-Pylm** upon progressive addition of **CB[7]** or **CB[8]**. (For the other guests refer to Section 4 in Supporting Information.) The initial line-broadening is attributed to site-exchange between free and intercalated guest and indirectly supports both the stoichiometry of the complexes and the high equilibrium constants of intercalation (Table 2): the resonance lines become sharp again after addition of 1.25 mol of **CB[7]** and 0.5 mol of **CB[8]**. All protons (aromatic and aliphatic) of **Me-Pylm** shift exactly the

Table 2. Equilibrium Constants (M^{-1}) per Scheme 1 from Data as in Figure 3 and Figures S2−S4 in Supporting Information

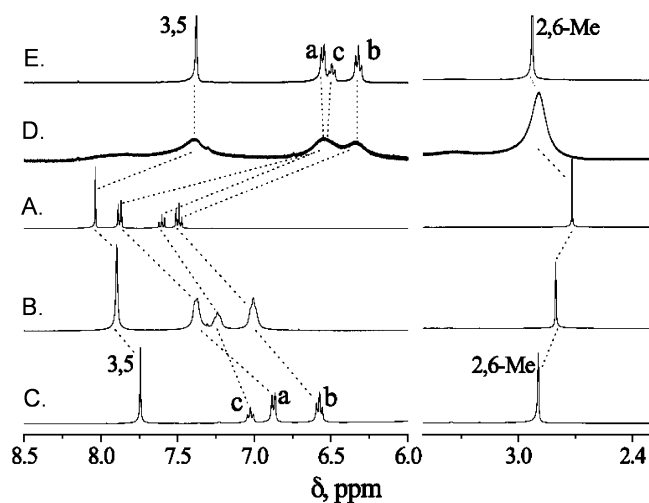| guest	$K_{[7]}$	$K_{[8],1}$	$K_{[8],2}$	$K_{[8],3}$
Me-Pylm	$(3 \pm 1) \times 10^5$	$(1.2 \pm 0.3) \times 10^4$	5.6×10^6	6.7×10^6
*i*Pr-Pylm	$(1 \pm 1) \times 10^5$	$(8 \pm 8) \times 10^4$	4.8×10^6	12×10^6
t-Bu-Pylm	$(8 \pm 3) \times 10^4$	$(4 \pm 4) \times 10^4$	1.7×10^5	5.7×10^4
Ph-Pylm	$(6 \pm 2) \times 10^4$	$(3 \pm 2) \times 10^4$	1.5×10^5	1.2×10^4

Figure 4. (A) ¹H NMR of **Me-Pylm** in unbuffered D$_2$O (pH ~2−4). (B, C) Plus 0.5 and 1.25 molar equiv of **CB[7]**. (D, E) Plus 0.25 and 0.5 molar equiv of **CB[8]**.

Figure 5. ¹H NMR of the four guests in unbuffered D$_2$O (pH ~2−4) after addition of 1.25 molar equiv of **CB[7]** or 0.5 molar equiv of **CB[8]**. Chemical shift changes are summarized in Figure 6.

same way in either host, and therefore the guest monomer in **CB[7]**, or **(Me-Pylm)$_2$** in **CB[8]** are positioned similarly in the two hosts, by placing the 4-phenyl group inside the cavity and leaving the methyl groups outside. It is noted that although it is known that pyrylium salts react with water faster in neutral media and slower in lower pHs (by nucleophilic attack at the 2- or 6-positions yielding 1,5-disubstituted-2-pentene-1,5-diones),[31] we have detected no quantitative decomposition by ¹H NMR within the duration of our experiments (≤1 h) and surprisingly no detectable decomposition for some guests (e.g., **Ph-Pylm**) even after 13 days in solution; in all cases no decomposition from complexed guests was detected either (see Figure S18 in Supporting Information). Thus, all studies were conducted in unbuffered solutions, whose pHs were measured in the 2−4 range, probably because of residual HCl carried over from the recrystallization of the hosts. Upon a reviewer's request, we also attempted to increase the pH by adding NaOD. The ¹H NMR spectra are included in Figure S18. As expected, all pyryliums decomposed within minutes at pH ≥ 7.00.

A similar pattern in the chemical shift change upon intercalation in **CB[7]** is also observed for **iPr-**, **t-Bu-**, and **Ph-Pylm** (Figure 5). Chemical shift changes upon complexation have been color-coded and cited in Figure 6. We observe that all 4-phenyl aromatic H's move upfield and hence sit inside the cavity, whereas aliphatic H's move downfield and hence are located outside near the rim O's. Interestingly, in the cases of **t-Bu-** and **Ph-Pylm**, H$_{3,5}$ move *downfield*, and that may be attributed to steric reasons, whereas bulky **t-Bu-** and Ph-substituents prevent those guests from sinking as deep in the cavity, leaving H$_{3,5}$ near the electric field of the rim O$_s$. That view needs to be moderated though by the fact that H$_{3,5}$ located outside the cavity become susceptible to interaction with H$_2$O, which also moves them downfield (see below).

Those conclusions are fully supported computationally. Starting from one **CB[7]** host and two *separated* guests (i.e., not in dimer form) outside the cavity, the M062X method yields negative potential energies and predicts local minima for both 1:1 and 2:1 complexes with **Me-**, **t-Bu-**, and **Ph-Pylm**, with the 2:1 complexes preferred at 0 K (Table 3). For **iPr-Pylm**, even starting with two **iPr-Pylm** inside **CB[7]**, one guest
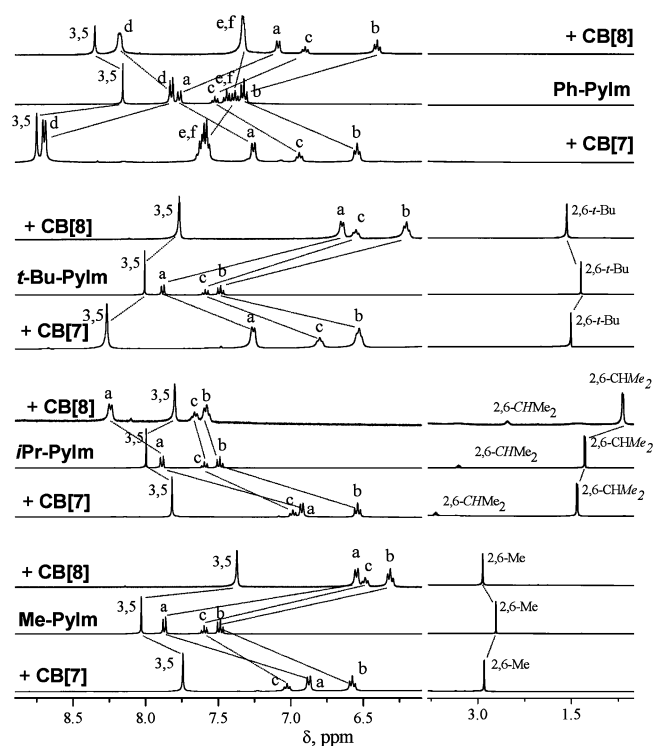
was always expelled. However, considering Gibbs free energies of complexation at 298 K, together with the fact that in the case of 1:1 complexes the remaining guests are free to dimerize, the 1:1 complexes are preferred for all guests (except for **Ph-Pylm**). The trend in the (all negative) ΔG^{298} values (Table 3) is **Me-** < **t-Bu-** < **iPr-** < **Ph-**, which mirrors the general trend of the K$_{[7]}$ values (in reverse order, of course): **Me-** > **iPr-** > **t-Bu-** > **Ph-**. (The B3LYP method disfavors two guests in **CB[7]** even at 0 K, and although it produces similar structures as M062X, the positive Gibbs free energies (tabulated in Section 7 of the Supporting Information) do not correspond to significant concentrations of any complexes, either 1:1 or 2:1, at 298 K.)

The preferred orientation of all four guests (shown along the ¹H NMR data in Figure 6) is with the 4-phenyl ring of the pyrylium moiety inside the **CB[7]** cavity, and the aromatic ring O$^+$ and counterion outside. In full agreement with the interpretation of the ¹H NMR data, **Me-Pylm** sits the deepest in the **CB[7]** host cavity (and is tipped over significantly in orientation, by 26.3°). **iPr-**, **t-Bu-**, and **Ph-Pylm** are progressively less tipped (12.7°, 9.4°, and 8.0°, respectively) and also do not enter as deeply. The sequence from deepest to most shallow is **Me-** (0.885) > **Ph-** (1.192) > **iPr-** (1.400) > **t-Bu-** (1.411), where in parentheses are the distances (in Å) of H$_c$'s from the bottom portal C=O's. Complete quantitative information and geometric parameters describing the position and orientation of the guests as well as the puckering distortions of the **CB[7]** host are provided in Section 7 of the Supporting Information. Consistent with the ¹H NMR interpretation, H$_{3,5}$ of **t-Bu-** and **Ph-Pylm** are outside the cavity, 0.837 and 0.601 Å, respectively, from the rim oxygen plane.

In the case of **CB[8]**, there are two stereochemical issues to be reconciled consistently: (a) the orientation of the dimer itself and (b) the orientation of the dimer in the cavity. In that
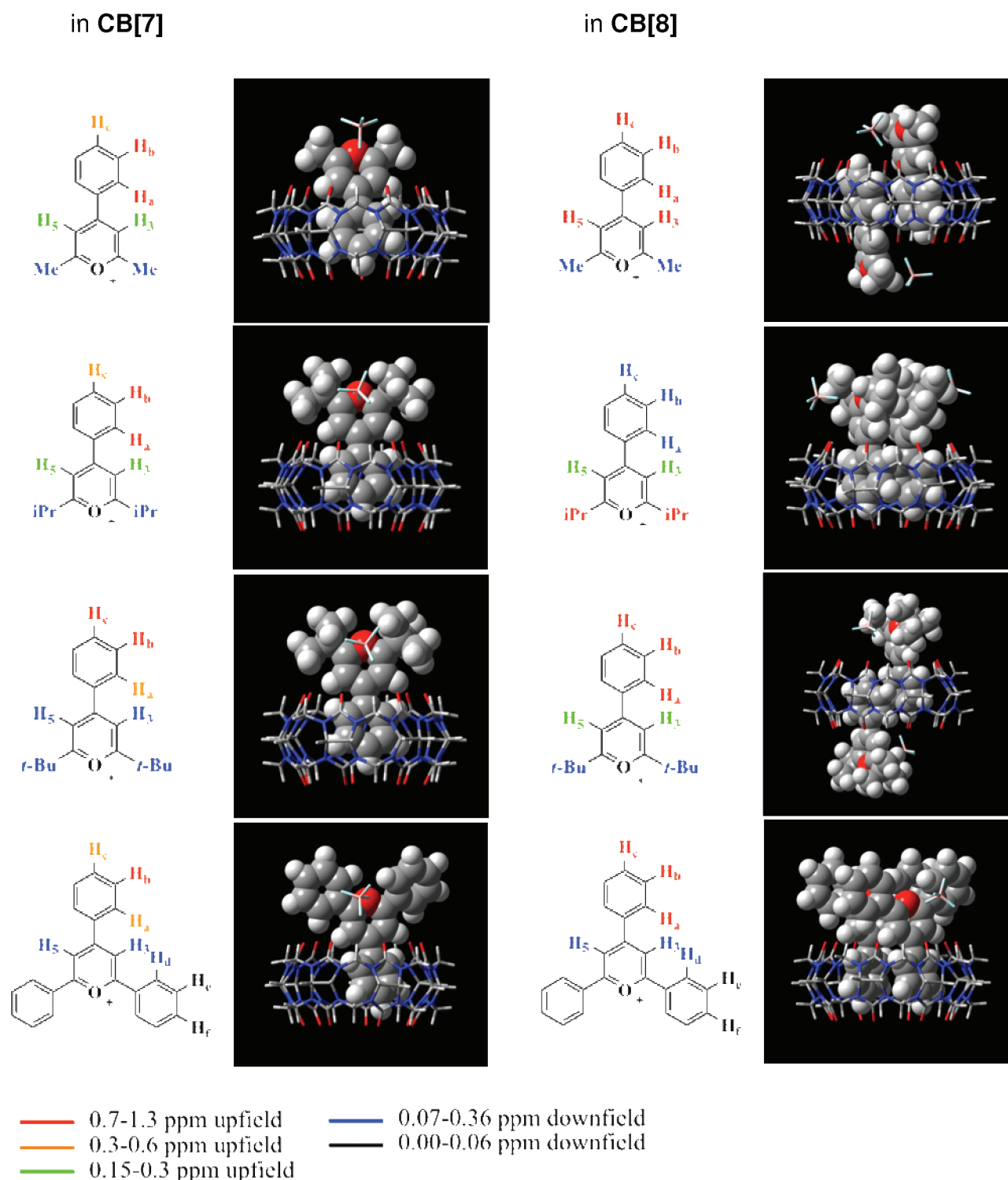
Figure 6. M062X/6-31G(d) optimized structures at 0 K for the guests shown at left. (The BF_4^- counteranions are included in wire-frame format.) Color-coding summarizes the ^{1}H NMR chemical shift changes upon intercalation relative to the free guests.

regard, the 4-phenyl ring H's of **Me-**, **t-Bu-**, and **Ph-Pylm** dimers show the same general pattern of chemical shift changes as in **CB[7]** (Figure 5), signifying a similar orientation, namely, with the 4-phenyl groups inside the cavity. An *upfield* shift of $H_{3,5}$ in the case of **t-Bu-Pylm** might signify either changes in the solvation shell (see below), or that the guest sits deeper in **CB[8]** than in **CB[7]**, in both cases reflecting the relative sizes

of the portals. (Again, color-coded chemical shift changes relative to the free guests are cited in Figure 6.)

Additional information in the stereochemical investigation of the complexes is provided by the ^{1}H NMR of the **CB[8]** host in the complexes (Figure 7). Antiparallel orientation of the guest dimers results in concerted puckering of the two (upper and lower) portals of **CB[8]**, while the two rims respond (stretch) differently when the two guests protrude through the

Table 3. Potential (ΔV) and Gibbs Free (ΔG^{298}) Energies (both in kcal mol^{-1}) of the Four Guests in CB[7] and CB[8] by the M062X/6-31G(d) Method[a]

	CB[7]				CB[8]			
	ΔV		ΔG^{298}		ΔV		ΔG^{298}	
	guest as monomer	guest as dimer	guest as monomer	guest as dimer	guest as monomer	guest as dimer	guest as monomer	guest as dimer
Me-Pylm[b]	−26.65	−45.18	−9.07[d]	−1.21	−23.08	−48.81	−7.04	−17.97
iPr-Pylm[b]	−22.65	e	−2.61[d]	e	−23.37	−50.48	−6.65	−16.88
iPr-Pylm[c]	−22.65	e	−2.61[d]	e	−23.37	−51.10	−6.65	−15.62
t-Bu-Pylm[b]	−21.33	−35.38	−3.24[d]	9.25	−20.11	−41.91	−4.67	−12.87
Ph-Pylm[c]	−22.34	−48.13	−0.01[d]	−1.75	−21.37	−55.96	−6.20	−19.90

[a]The zero energy level represents two separated guests (i.e., not in dimer form) separated from the corresponding host. [b]Antiparallel alignment as in the free guest dimer. [c]Parallel (side-by-side) alignment. [d]Calculated taking into consideration that the second guest remains outside the cavity and is free to dimerize with ΔG^{298} provided in Table 1. [e]Second guest was expelled.
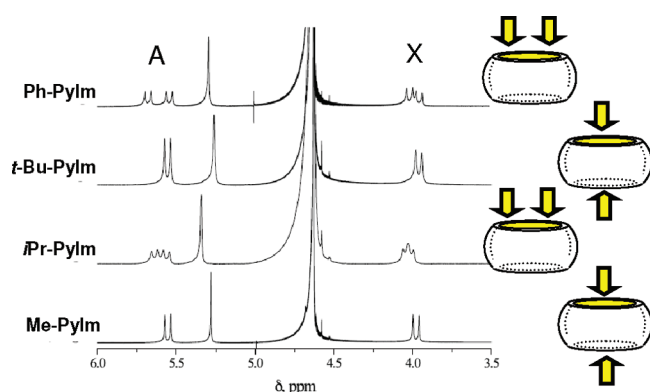

Figure 7. ^{1}H NMR (D$_2$O) of CB[8] after addition of 2 mol of the guests at left. Arrows show the direction of intercalation of the two guests suggested by the host D_{8h} symmetry breakdown. Upon asymmetric intercalation of **iPr-** and **Ph-Pylm** the CH$_A$H$_X$ rim protons are no longer equivalent at the two rims. Signal broadening is attributed to puckering of the host (see Table S21 in Supporting Information).

same side (similarly to the ^{1}H NMR of **CB[7]** hosting only one guest; see Figure S17 in Supporting Information). Thus, data in Figure 7 show that the D_{8h} symmetry of free **CB[8]** is nearly retained in **(Me-Pylm)$_2$@CB[8]** and **(t-Bu-Pylm)$_2$@CB[8]** but breaks down more significantly in the case of **(iPr-Pylm)$_2$@CB[8]** and **(Ph-Pylm)$_2$@CB[8]**, suggesting that **Me-**, **t-Bu-**, and **Ph-Pylm** enter the cavity in their preferred free dimer orientations: antiparallel in **(Me-Pylm)$_2$@CB[8]** and **(t-Bu-Pylm)$_2$@CB[8]** and parallel in **(Ph-Pylm)$_2$@CB[8]**, consistent also with its crystal structure.[17] In the latter case, as mentioned in the Introduction, two modes for insertion of the **(Ph-Pylm)$_2$** dimer in the **CB[8]** cavity have been identified: through the 4- but also through one of the 2-phenyl groups (always the guest dimer being in the parallel configuration). In solution, the later mode of insertion is not supported by ^{1}H NMR, but the possibility of placing the 2-phenyl groups inside the cavity (instead of those at the 4-position) might be important in relation to the orientation of the **(iPr-Pylm)$_2$** in **CB[8]** discussed below.

The case of **(iPr-Pylm)$_2$@CB[8]** commands special attention. The symmetry breakdown noted in Figure 7 suggests that the two guests might assume a parallel orientation, which is *not* the preferred orientation of the free dimer. Further, the chemical shifts of H$_{3,5}$ as well as those of the iPr groups move upfield, while the chemical shifts of H$_a$, H$_b$, and H$_c$ move downfield (see Figure 5 and summary in Figure 6). This trend

is opposite to what is observed with the other guests or with **iPr-Pylm** itself in **CB[7]** and difficult to reconcile consistently with the 4-phenyl group inside the **CB[8]** cavity. Nevertheless, all chemical shift changes for the **iPr-Pylm** guest in **CB[8]** are profound and systematic and need to be considered collectively.

Thus first, M062X calculations (Table 3) clearly support the 2:1 stoichiometry for all four guests in **CB[8]**, even when subsequent dimerization of excess monomers with 1:1 guest-**CB[8]** complexes is considered. Regarding orientation, it was not assumed that guests maintain their preferred dimer structures (antiparallel for **Me-**, **iPr-** and **t-Bu-Pylm**, and parallel for **Ph-Pylm**), but that was found to be the lowest *free-energy* configuration in all cases, presumably realizing benefit from interactions of the guests both between themselves and with the host. In the case of **iPr-Pylm**, the lowest energy 0 K structure aligns the two guests parallel to each other (Figure 6). With thermochemical corrections though, calculated ΔG^{298} slightly favors the antiparallel configuration (i.e., maintaining the preferred free dimer configuration), but the difference is certainly within the uncertainty of the reported energies (just 1.26 kcal mol^{-1}, Table 3). For comparison, parallel guest configurations calculated with the M062X method for **(Me-Pylm)$_2$@CB[8]** and **(t-Bu-Pylm)$_2$@CB[8]** are disfavored relative to the preferred antiparallel guest orientation by about 3.0 and 7.2 kcal/mol, respectively. (For B3LYP, the 0 K potential energies show the 2:1 complexes to be the most stable (see Supporting Information), but as in the case of **CB[7]**, ΔG^{298} values predict no significant complex concentrations at 298 K. The B3LYP method also favors a head-to-tail arrangement of the two **Ph-Pylm** guests, rather than the π-stacking arrangement predicted by M062X and identified crystallographically.[17]) Again, quantitative information including B3LYP results and geometric parameters are provided in Supporting Information.

Although the calculations above suggest that a parallel arrangement of **iPr-Pylm** in **(iPr-Pylm)$_2$@CB[8]** might not be disfavored, no energetically competitive structure was located with the iPr groups entering the cavity. In fact, forcing those groups into **CB[8]** leads to strong destabilization (by ~40 kcal mol^{-1}). Clearly, there are unaccounted factors for the inverted ^{1}H NMR data for that complex. Thus, we turned into correlating experimental ^{1}H NMR data with calculated chemical shifts based on the optimized structures above. For this, we started with the GIAO method[32] and the B3LYP functional including implicit water solvation with the PCM model for the simplest guest by itself, **Me-Pylm**. Chemical shifts were

computed relative to a calculated TMS reference at the same level of theory. Detailed data are provided in Supporting Information. Experimentally, the aromatic proton chemical shifts of **Me-Pylm** fall in the 8.5−7.5 ppm range in the order: $H_{3,5} > H_a > H_c > H_b$ (Figures 4 and 5). B3LYP calculations for either the **Me-Pylm** monomer or dimer yield chemical shifts in the same region, but in the order $H_a > H_c > H_b > H_{3,5}$. Then, it was determined that the shift of the $H_{3,5}$ protons is sensitive to explicit solvation effects (in particular a water molecule is stabilized bridging the $H_{3,5}$ and H_a protons). Thus, subsequent calculations for optimized 0 K structures including two explicit water molecules produced shifts in the experimentally observed order but brought the $H_{3,5}$ protons too far downfield (~9 ppm).[33] The importance of explicit solvation and finite temperature effects for reliable ^{1}H NMR calculations has been noted previously.[34−37] In that context, Born−Oppenheimer Molecular Dynamics (BOMD) simulations including 30 explicit water molecules in addition to the PCM implicit solvent model were run at 298 K with the B3LYP/6-31G(d) method within the Gaussian 09 software package[24] generating snapshots of the **Me-Pylm** monomer at 1 ps intervals. Those results are promising in terms of moderating the shift of the $H_{3,5}$ protons and reproduce the experimental shifts for **Me-Pylm** satisfactorily: δ (ppm experimental; ppm computed) $H_{3,5}$ (8.03; 8.23); H_a (7.88; 8.08); H_b (7.48; 7.70); H_c (7.60; 7.85); H_{Me} (2.71; 2.81) (for more details, see Table S22 in Supporting Information). Unfortunately though, that approach is too computationally costly to apply in a statistically meaningful way to the larger guest−host complexes. Nevertheless, those results underline the fact that closely associated water molecules may not only modify the guest structure (and influence, e.g., diffusion dynamics) but most importantly introduce non-bonding interactions that in turn influence the energetics of the entire interaction with the host. The lack of explicit solvation must be considered as an additional source of uncertainty in our calculations and is likely significant enough to potentially become a deciding factor in preferred host−guest structures, particularly in the case of $(i\mathbf{Pr\text{-}Pylm})_2@\mathbf{CB[8]}$ where the energies of two contending structures are so close.

CONCLUSION

The stereochemistry of host−guest complexes is extremely important for technology based on molecular recognition as in supramolecular protection, separations, and optoelectronic devices. The 2,6-disubstituted-4-phenylpyrylium/$\mathbf{CB}[x]$ system has allowed systematic variation of the factors that control stereochemistry. Those include an interplay between the size, flexibility, and hydrophobicity of the $\mathbf{CB}[x]$ cavity on one hand, and the size and solvation of the guest on the other. Specifically, hydrophobic interactions are a major driving force for complexation, as all four guests give up favorable π-stacking dimerization in solution (and energy equal to that in their J-aggregates, 5.5−7.6 kcal mol^{-1}) in order to enter $\mathbf{CB[7]}$ as monomers. In $\mathbf{CB[8]}$, with cavity-size restrictions relaxed, **Me-**, **t-Bu-**, and **Ph-Pylm** enter as dimers in the same orientation as in their free dimers, thus retaining the π-stacking interactions, while they also realize hydrophobic stabilization by placing their 4-phenyl groups in the cavity. Meanwhile, iPr groups are significantly hydrophobic but less bulky than t-Bu- or Ph-. That may indicate a surprising arrangement in which a **iPr-Pylm** dimer places the i-Pr groups into the cavity, consistent with the observed trends in ^{1}H shifts, but disfavored by calculations. The only possible way for $(i\mathbf{Pr\text{-}Pylm})_2$ to place both iPr groups in

the $\mathbf{CB[8]}$ cavity and simultaneously realize π-interactions between the 4-phenyl groups is by assuming a parallel orientation, confirmed by ^{1}H NMR of the host and taken as an indirect evidence for the unexpected placement of the iPr groups in the cavity. Conceivably, in that arrangement, other resonance forms of pyrylium (e.g., a "quinone"-like diene structure with the positive charge at the c-position of the 4-phenyl group) may be important, while the stereochemistry of $(i\mathbf{Pr\text{-}Pylm})_2@\mathbf{CB[8]}$ is determined not only by hydrophobic and π-interactions but also by solvation of the $H_{3,5}$, which remain outside the cavity. Those explicit solvation effects were not accounted for in the structures shown in Figure 6 and were revealed only by ^{1}H NMR simulations. A similar orientation with $(t\mathbf{\text{-}Bu\text{-}Pylm})_2@\mathbf{CB[8]}$ and $(\mathbf{Ph\text{-}Pylm})_2@\mathbf{CB[8]}$ is not observed, signifying that the stereochemistry of those complexes is determined by the relative sizes of the 2,6-substituents and the portals.

Overall, explicit interactions with the solvent in host−guest complexes should not be underestimated. Monocationic guests are suitable for assessing the relative importance of all factors involved. N-Methyl-4-benzoylpyridinium mentioned in the Introduction represents a case at one extreme, whereas solvent (water) is directly involved with the guest in a keto/*gem*-diol equilibrium, which is shifted toward the keto form by the hydrophobic interaction of the 4-benzoyl group with the $\mathbf{CB[7]}$ cavity, underlining the importance of the latter in the orientation of the guest. Here, the more subtle case of $(i\mathbf{Pr\text{-}Pylm})_2@\mathbf{CB[8]}$ suggests that explicit solvation of groups staying outside the cavity may be also very important in fine-balance with the hydrophobic interactions of the groups placed in the cavity for determining stereochemistry.

■ EXPERIMENTAL SECTION

$\mathbf{CB[7]}$ was available from previous work.[13] $\mathbf{CB[8]}$ was purchased from Sigma-Aldrich. HPLC-grade water for spectrophotometric titrations was purchased from Fisher Scientific.

2,6-Dimethyl-4-phenylpyrylium Tetrafluoroborate (Me-Pylm). Prepared by the method of Breit et al.[18] The product was recrystallized from water. Mp 202−203 °C (lit.[18] mp 196 °C); ^{1}H NMR (D$_2$O) δ (ppm) 8.03 (s, 2H, $H_{3,5}$), 7.88 (d, 2H, $J_{a,b}$ = 7.5 Hz, H_a), 7.48 (t (indiscernible dd), 2H, $J_{ab} = J_{bc}$ = 7.5 Hz, H_b), 7.60 (t, 1H, J_{bc} = 7.5 Hz, H_c), 2.71 (s, 6H, CH$_3$); HRMS calcd for C$_{13}$H$_{13}$O$^+$ 185.09609, found 184.93177.

2,6-Diisopropyl-4-phenylpyrylium Tetrafluoroborate (iPr-Pylm). Prepared by the method of Breit et al.[18] The product was recrystallized from CH$_2$Cl$_2$/hexane. Mp 182−184 °C (lit.[18] mp 178 °C; lit.[38] mp 181−183 °C); ^{1}H NMR (D$_2$O) δ (ppm) 7.99 (s, 2H, $H_{3,5}$), 7.87 (d, 2H, J_{ab} = 7.5 Hz, H_a), 7.49 (t (indiscernible dd), 2H, J_{ab} = J_{bc} = 7.5 Hz, H_b), 7.59 (t, 1H, J_{bc} = 7.5 Hz, H_c), 3.31 (sept, 1H, J = 6.9 Hz, CH), 1.29 (d, 6H, J = 6.9 Hz, CH$_3$); HRMS calcd for C$_{17}$H$_{21}$O$^+$ 241.15869, found 241.02529.

2,6-Di-t-butyl-4-phenylpyrylium Tetrafluoroborate (t-Bu-Pylm). Prepared by the method of Lin and Schuster.[19] The product was recrystallized from CH$_2$Cl$_2$/hexane. Mp 218−220 °C (lit.[19] mp 223 °C); ^{1}H NMR (D$_2$O) δ (ppm) 8.01 (s, 2H, $H_{3,5}$), 7.88 (d, 2H, J_{ab} = 7.5 Hz, H_a), 7.48 (t (indiscernible dd), 2H, J_{ab} = J_{bc} = 7.5 Hz, H_b), 7.59 (t, 1H, J_{bc} = 7.5 Hz, H_c), 1.31 (s, 18H, CH$_3$); HRMS calcd for C$_{19}$H$_{25}$O$^+$ 269.18999, found 269.06000.

2,4,6-Triphenylpyrylium Tetrafluoroborate (Ph-Pylm). Purchased from Sigma-Aldrich. Mp 249−250 °C (lit.[38] mp 250−252 °C); ^{1}H NMR (D$_2$O) δ (ppm) 8.15 (s, 2H, $H_{3,5}$), 7.82 (d, 4H, J_{de} = 7.4 Hz, H_d), 7.77 (d, 2H, J_{ab} = 7.4 Hz, H_a), 7.37−7.54 (m, 9H, ArH); HRMS calcd for C$_{23}$H$_{17}$O$^+$ 309.12739, found 309.02389.

General Methods. ^{1}H NMR spectra were obtained with a 400 MHz Varian Unity Inova NMR instrument in D$_2$O, were referenced to the residual solvent (4.63 ppm), and are reported as parts per million

(ppm) from TMS (δ). High resolution mass spectra (HRMS) were obtained with a ThermoFinnigan TSQ7000 triple-quadrupole mass spectrometer (ThermoFinnigan, San Jose, CA). Freshly made samples were infused into the electrospray (ESI) source at 10 μL min^{-1} using a 500 μL Gastight syringe (Hamilton, Reno, NV) in a Pump 11 syringe pump (Harvard Apparatus, Holliston, MA). The electrospray needle voltage was 4.5 kV and the heated inlet capillary temperature was 250 °C. All other voltages were optimized to maximize ion transmission and minimize unwanted fragmentation (as determined during the regular tuning and calibration of the instrument). Nitrogen sheath gas was provided at 80 psi from a Dewar of liquid nitrogen. Data are reported at a mass resolution of 1 part in 100,000. Binding constants were determined spectrophotometrically (Beckman DU 640B spectrophotometer) keeping the pyrylium salt concentration constant and varying the concentration of the host (**CB[7]** or **CB[8]**). Plots of the absorbance at a specific wavelength versus host concentration were fitted using nonlinear regression analysis and the appropriate mechanism.[30] Each experiment was conducted twice, and the reported equilibrium constants are averages. Raw data, equations, and calculations are provided in Section 3 of the Supporting Information. X-ray diffraction (XRD) analysis of **Me-Pylm** was conducted on a Bruker Smart Apex diffractometer using SMART software.[39] Suitable crystals grown in water were selected and mounted on a glass fiber using epoxy glue. Intensity data sets were collected at 123 K employing a scan of 0.3° in ω with an exposure time of 20 s per frame. Cell refinement and data reduction were carried out with SAINT.[40] Absorption correction was carried out with SADABS software package.[40] The structure was solved by direct methods using SHELXS-97 and difference Fourier syntheses.[41] Full-matrix least-squares refinement against |F^2| was carried out using the SHELXTL-PLUS suit of programs.[40] All non-hydrogen atoms were refined anisotropically, while H-atoms were placed geometrically and held in the riding mode during the final refinement. Optimized structures were located using two different density functional theory (DFT) methods, the B3LYP and M062X functionals and the 6-31G(d) basis set. Each guest molecule was accompanied by a BF$_4^-$ counterion, and the effects of solvation (water) were included using the Polarizable Continuum Model (PCM) as implemented in the Gaussian 09 package.[24] Optimizations were performed in Cartesian coordinates with an *ultrafine* integration grid and initiated with a calculated Hessian matrix.

ASSOCIATED CONTENT

Ⓢ Supporting Information

Job's plots; UV−vis absorption data and analysis for guest dimerization constants and binding constants with **CB[7]** and **CB[8]**; ^{1}H NMR data including guest stability studies; Computational section with dimerization of guests, intercalation in the two hosts, geometric parameters of the complexes, ^{1}H NMR calculations, and tables of atom coordinates and absolute energies; crystallographic data for **Me-Pylm** including a CIF file. This material is available free of charge via the Internet at http://pubs.acs.org.

AUTHOR INFORMATION

Corresponding Author

*cslevent@mst.edu; dawesr@mst.edu; leventis@mst.edu

Notes

The authors declare no competing financial interest.

ACKNOWLEDGMENTS

REFERENCES

(1) Lee, J. W.; Samal, S.; Selvapalam, N.; Kim, H.-J.; Kim, K. *Acc. Chem. Res.* **2003**, *36*, 621−630.

(2) Kim, K.; Selvapalam, N.; Oh, D. H. *J. Inclusion Phenom. Macrocyclic Chem.* **2004**, *50*, 31−36.

(3) It should be noted though that there is a discrepancy in the literature concerning the cavity height: references 1 and 2 list 9.1 Å, however, crystal structures for **CB[7]** and **CB[8]** given as Supporting Information in reference 2, or for the complex of a ferrocene derivative with **CB[7]**,[4] confirm that the O-O distance is ∼6.1 Å. Most DFT calculations are also in agreement, giving O-O distance in the range of 6.0 - 6.2 Å.[5,6] In another computational study, however, the cavity height was reported not as the distance between O-atom nuclei, but rather as the distance between critical points of the calculated molecular electrostatic potential (MESP); that distance ranges from 7.35 Å for **CB[5]** to 7.70 Å for **CB[8]**.[7] Unfortunately, when those calculations were referenced later, the data were inadvertently converted into units of bohr and reported as ∼14 Å.[8]

(4) Jeon, W. S.; Moon, K.; Park, S. H.; Chun, H.; Ko, Y. H.; Lee, J. Y.; Lee, E. S.; Samal, S.; Selvapalam, N.; Rekharsky, M. V.; Sindelar, V.; Sobransingh, D.; Inoue, Y.; Kaifer, A. E.; Kim, K. *J. Am. Chem. Soc.* **2005**, *127*, 12984−12989.

(5) Márquez, C.; Hudgins, R. R.; Nau, W. M. *J. Am. Chem. Soc.* **2004**, *126*, 5806−5816.

(6) Buschmann, H.-J.; Wego, A.; Zielesny, A.; Schollmeyer, E. *J. Inclusion Phenom. Macrocyclic Chem.* **2006**, *54*, 85−88.

(7) Pinjari, R. V.; Gejji, S. P. *J. Phys. Chem. A* **2008**, *112*, 12679−12686.

(8) Pinjari, R. V.; Khedkar, J. K.; Gejji, S. P. *J. Inclusion Phenom. Macrocyclic Chem.* **2010**, *66*, 371−380.

(9) Kim, H.-J.; Jeon, W. S.; Ko, Y. H.; Kim, K. *Proc. Nat. Acad. Sci. U.S.A.* **2002**, *99*, 5007−5011.

(10) Sindelar, V.; Moon, K.; Kaifer, A. E. *Org. Lett.* **2004**, *6*, 2665−2668.

(11) Moon, K.; Kaifer, A. E. *Org. Lett.* **2004**, *6*, 185−188.

(12) Rawashdeh, A.-M. M.; Thangavel, A.; Sotiriou-Leventis, C.; Leventis, N. *Org. Lett.* **2008**, *10*, 1131−1134.

(13) Thangavel, A.; Rawashdeh, A.-M. M.; Sotiriou-Leventis, C.; Leventis, N. *Org. Lett.* **2009**, *11*, 1595−1598.

(14) Jeon, W. S.; Kim, H.-J.; Lee, C.; Kim, K. *Chem. Commun.* **2002**, 1828−1829.

(15) Manoj, N.; Gopidas, K. R. *Phys. Chem. Chem. Phys.* **1999**, *1*, 2743−2748.

(16) Montes-Navajas, P.; Teruel, L.; Corma, A.; Garcia, H. *Chem.—Eur. J.* **2008**, *14*, 1762−1768.

(17) Montes-Navajas, P.; Garcia, H. *J. Phys. Chem. C* **2010**, *114*, 2034−2038.

(18) Breit, B.; Winde, R.; Mackewitz, T.; Paciello, R.; Harms, K. *Chem.—Eur. J.* **2001**, *7*, 3106−3121.

(19) Lin, Z.; Schuster, G. B. *J. Org. Chem.* **1994**, *59*, 1119−1125.

(20) Osaka, I.; Kondou, M.; Selvapalam, N.; Samal, S.; Kim, K.; Rekharsky, M. V.; Inoue, Y.; Arakawa, R. *J. Mass Spectrom.* **2006**, *41*, 202−207.

(21) Gadde, S.; Batchelor, E. K.; Weiss, J. P.; Ling, Y.; Kaifer, A. E. *J. Am. Chem. Soc.* **2008**, *130*, 17114−17119.

(22) Bordello, J.; Reija, B.; Al-Soufi, W.; Novo, M. *ChemPhysChem* **2009**, *10*, 931−939.

(23) Miraldi, E. R.; Thomas, P. J.; Romberg, L. *Biophys. J.* **2008**, *95*, 2470−2486.

(24) Frisch, M. J.; Trucks, G. W.; Schlegel, H. B.; Scuseria, G. E.; Robb, M. A.; Cheeseman, J. R.; Scalmani, G.; Barone, V.; Mennucci, B.; Petersson, G. A.; Nakatsuji, H.; Caricato, M.; Li, X.; Hratchian, H. P.; Izmaylov, A. F.; Bloino, J.; Zheng, G.; Sonnenberg, J. L.; Hada, M.; Ehara, M.; Toyota, K.; Fukuda, R.; Hasegawa, J.; Ishida, M.; Nakajima, T.; Honda, Y.; Kitao, O.; Nakai, H.; Vreven, T.; Montgomery, J. A., Jr.; Peralta, J. E.; Ogliaro, F.; Bearpark, M.; Heyd, J. J.; Brothers, E.; Kudin, K. N.; Staroverov, V. N.; Kobayashi, R.; Normand, J.; Raghavachari, K.; Rendell, A.; Burant, J. C.; Iyengar, S. S.; Tomasi, J.; Cossi, M.; Rega, N.; Millam, N. J.; Klene, M.; Knox, J. E.; Cross, J.

B.; Bakken, V.; Adamo, C.; Jaramillo, J.; Gomperts, R.; Stratmann, R. E.; Yazyev, O.; Austin, A. J.; Cammi, R.; Pomelli, C.; Ochterski, J. W.; Martin, R. L.; Morokuma, K.; Zakrzewski, V. G.; Voth, G. A.; Salvador, P.; Dannenberg, J. J.; Dapprich, S.; Daniels, A. D.; Farkas, Ö.; Foresman, J. B.; Ortiz, J. V.; Cioslowski, J.; Fox, D. J. *Gaussian 09*, Revision B.01; Gaussian, Inc.: Wallingford, CT, 2010.

(25) Becke, A. D. *J. Chem. Phys.* **1993**, *98*, 5648−5652.

(26) Zhao, Y.; Truhlar, D. G. *Acc. Chem. Res.* **2008**, *41*, 157−167.

(27) Milov, A. A.; Starikov, A. G.; Gridin, M. K.; Minyaev, R. M. *Russ. J. Gen. Chem.* **2007**, *77*, 1373−1385.

(28) (a) Job, P. *Ann. Chim. Appl.* **1928**, *9*, 113−203. (b) Krunz, M. M.; Pfendt, L. B. *Microchem. J.* **1983**, *28*, 162−167. (c) Cartwright, H. M. *Microchem. J.* **1986**, *34*, 313−318. (d) Schneider, H.-J.; Yatsimirsky, A. *Principles and Methods in Supramolecular Chemistry*; John Wiley & Sons: New York, NY, 2000; p 149. (e) Gil, V. M. S.; Oliveira, N. C. *J. Chem. Educ.* **1990**, *67*, 473−478.

(29) (a) Jayataj, N.; Maddipatla, M. V. S. N.; Prabhakar, R.; Jockusch, S.; Turro, N. J.; Ramamurthy, V. *J. Phys. Chem. B* **2010**, *114*, 14320−14328. (b) Mu, L.; Yang, X.-B.; Xue, S.-F.; Zhu, Q.-J.; Tao, Z.; Zeng, X. *Anal. Chim. Acta* **2007**, *597*, 90−96.

(30) Connors, K. A. *Binding Constants, The Measurement of Molecular Complex Stability*; John Wiley and Sons, Inc.: New York, 1987.

(31) Williams, A. *J. Am. Chem. Soc.* **1971**, *93*, 2733−2737.

(32) (a) Ditchfield, R. *Mol. Phys.* **1974**, *27*, 789−807. (b) Wolinski, K.; Hilton, J. F.; Pulay, P. *J. Am. Chem. Soc.* **1990**, *112*, 8251−8260.

(33) Analogous ^{1}H NMR calculations using the M062X functional produced qualitatively similar results, but with ^{1}H shifts ∼1 ppm further downfield (in worse agreement with experiment).

(34) Cossi, M.; Crescenzi, O. *J. Chem. Phys.* **2003**, *118*, 8863−8872.

(35) Benzi, C.; Crescenzi, O.; Pavone, M.; Barone, V. *Magn. Reson. Chem.* **2004**, *42*, S57−S67.

(36) Aidas, K.; Møgelhøj, A.; Kjær, H.; Nielsen, C. B.; Mikkelsen, K. V.; Ruud, K.; Christiansen, O.; Kongsted, J. *J. Phys. Chem. A* **2007**, *111*, 4199−4210.

(37) Dračínský, M.; Kaminský, J.; Bouř, P. *J. Phys. Chem. B* **2009**, *113*, 14698−14707.

(38) Katritzky, A. R.; Rubio, O. *J. Org. Chem.* **1984**, *49*, 448−454.

(39) *SMART*; Bruker AXS Inc.: Madison, WI, 2002.

(40) *SAINT* and *SADABS*; Bruker AXS Inc.: Madison, WI, 2008.

(41) Sheldrick, G. M. *Acta Crystallogr.* **2008**, *A64*, 112−122.